Solid Freeform Fabrication 2024: Proceedings of the 35th Annual International
Solid Freeform Fabrication Symposium – An Additive Manufacturing Conference
Reviewed Paper

PROCESS LIMITATION FOR POWDER BED FUSION WITH LASER BEAM MULTIPLICATION

F. J. O. Spieth[a], T. Heeling[a], and H.-C. Moehring[b]

[a]Robert Bosch Manufacturing Solution GmbH, Wernerstraße 51, 70469 Stuttgart, Germany
[b]Institute for Machine Tools, University Stuttgart, Holzgartenstraße 17, 70174 Stuttgart, Germany

Abstract

The necessity to improve the productivity per laser in powder bed fusion is driven by demands for increasing build rates, combined with high resolution and process requirements. One promising solution is the use of a beam splitter to build multiple parts with a single laser scanner system at once, utilising the full available laser power available in today's single mode laser systems. However, due to its specific characteristics, this approach leads to limitations regarding part size, process window, build job layout, geometric tolerances, and machine specifications. This publication aims to investigate the influence of process boundaries on viable applications. In particular, the effect of beam splitting-related optical errors and the effect of shielding gas flow direction are analysed. The position dependent intensity and the superposition of effects are evaluated in terms of future boundaries on the technical implementation. Additionally, potential compensation methods for mitigating the detected limitations are discussed.

Introduction

The use of beam splitters to improve the productivity in powder bed fusion with laser beam for metals (PBF-LB/M) is part of ongoing research [1,2]. Nevertheless, the optical errors inherent to beam splitting in PBF-LB/M and the resulting limitations for the process compared to a conventional process need further research. Especially for the use in high separation angle beam splitting PBF-LB/M because of the bigger influence of the inherent optical errors [3]. The inherent optical errors from the use of a diffractive optical element (DOE) result in three dimensional position errors and thereby defocus of the side beams on the build plate [4]. These influences especially for large spot distances <30 mm is not specifically analysed in current research yet.

The two main effects, defocus and intercube fume interaction must be investigated for a better understanding of the resulting process limits for a PBF-LB/M process with a high separation angle beam splitter. While the center beam remains unchanged, the side beams show a defocus depending on the target position of the center beam. The defocus of the laser beam in PBF-LB/M has significant effects on the melt pool width and depth [5]. Yet if the intensity is below a certain limit due to defocus, a decrease in part density is to be expected, due to lack of fusion porosity [6]. While the defocus of the laser beam can lead to lower build quality, it can be used to improve the process e. g. by decreasing the amount of spatter from the melt pool with larger beam diameters [7] or as an additional parameter in the active control of the process to influence melt pool width, cooling rates and absorption of the laser beam [8]. Additionally, the effects of the shielding gas flow are investigated in the presented work. The interaction of the laser beam with byproducts of

the process results in its reflection, dispersion, and absorption, and thereby an attenuation and defocus of the beam. In order to minimize these unwanted interactions, an optimal shielding gas flow is used for transporting the byproducts efficiently away from the process area without turbulences [9–11]. This is best achieved with a homogenous shielding gas flow with a low oxygen content for better densities and less defects in the build parts [12,13]. Furthermore, the angle between the shielding gas flow and the scanning process is crucial in controlling the surface roughness of printed specimens [14]. In addition to the negative effects of process fumes on the laser beam, spatter from the process can result in elevated surface roughness or the formation of pores in the parts, due to the presence of attached or embedded unmolten particles [15].

While all these effects take place in a single beam process, a multi-beam process, independent of the origin of the beams, increases the number of influences from fume and spatter. Now the beam can be scattered and absorbed not only by its own process byproducts, but by those of other simultaneous operating beams in its vicinity. The greatest effects are most likely to occur with parts positioned in a fume propagation dependent cone downstream of another laser beam operating simultaneously. [16]

In summary an influence from the defocus of the side beams and the interaction of the laser beam with the byproducts of the simultaneous beams is to be expected on the build quality in the form of more pores and a greater surface roughness. Nevertheless, some effects concerning the defocus might reduce the byproducts due to lower peak intensities in the wider and flatter melt pools leading to lower velocities of melt pool streams resulting in lower chances for spatter and thereby lower emissions. Therefore, an investigation is necessary on the quantitative influence on the resulting process limits for the presented PBF-LB/M with large separation angle beam splitting.

Materials and Methods

The experiments are conducted using a self-built laboratory machine with a commercially available 3D optic setup as shown in Figure 1. A continuous wave laser with a wavelength of 1070 µm and a beam focus diameter of 72 µm is used. A one-dimensional 3x1 DOE-based beam splitter is implemented, resulting in a working plane spot distance of 39.8 mm. For better understanding, the beams and the respective parts are labelled with the respective algebraic sign of the order number, with the center beam identified as order number 0 with no sign and the side beams as either order number -1 with a minus sign or order number 1 with a plus sign, depending on the coordinate direction.

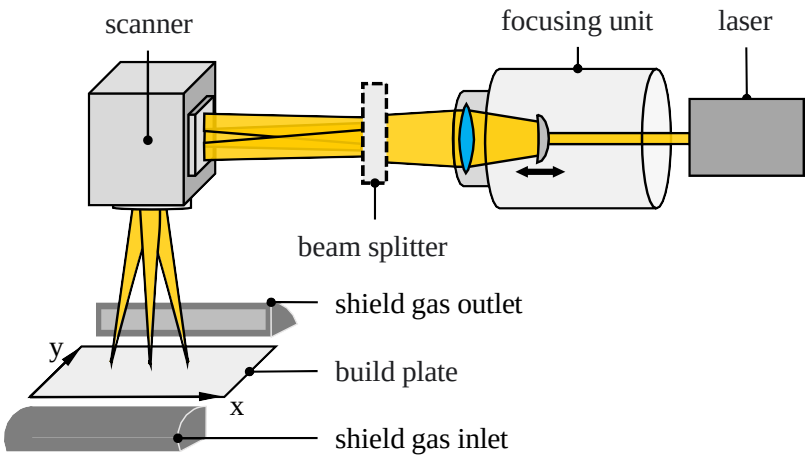

Figure 1: Overview of the optical setup of the laboratory PBF-LB/M machine

Argon is used as a shielding gas and for the creation of the inert atmosphere of the process chamber enabling an oxygen content below 0.3%. In an effort to better evaluate the influences of the shielding gas flow on the samples, the velocity of the shielding gas flow is measured over the build plate. The results above the build plate average 1.91 m/s in a height of 3 mm and 1.42 m/s in a height of 35 mm. The detailed results for the measurements with a discretisation of 20 mm for x and y axis are depicted in Figure 2.

Interpreting the measurements, an asymmetric distribution of shielding gas flow velocity for the positive and negative x- direction is observed for 3 mm height. This disparity shows a difference in average for the left and right side of 0.2 m/s. Due to the fact, that this difference is low compared to the average velocity and this behaviour is not visible for the velocity in 35 mm height, it is not further investigated in this work. In addition to that, is it important to recognize that the velocity for 3 mm height and $y \geq 40$ mm is drastically lower with an average of 1.05 m/s than the rest of the build plate. Therefore, the cubes build at positions of $y \geq 40$ are analysed separately because an insufficient evacuation of the process byproducts is to be expected.

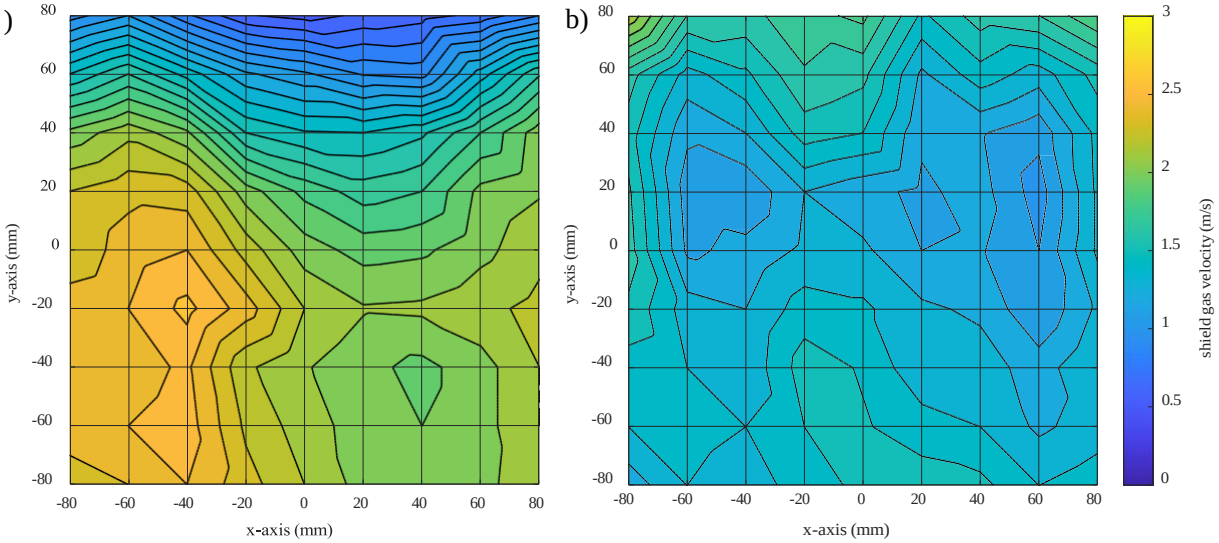

Figure 2: Shielding gas flow velocity distribution in a) 3 mm and b) 35 mm height above the build plate

In order to quantitatively evaluate the influence of the focus error, the error has to be measured for every position of the to be built cubes. This is achieved by measuring the focal level analysing focal rows on anodized aluminium plates. High-resolution images of these markings are used to calculate the focal level with an accuracy of 0.2 Rayleigh lengths. In the subsequent step, these results are combined with a measured caustic of the laser beam and used to calculate the resulting focus diameter DD from the position depended focus error ΔDD_{xyv} and the focus diameter of the center beam $DD_{0,0}$ in the origin of the build plate with $DD = \left(\frac{\Delta DD_{xyv}}{DD_{0,0}} + 1\right) * 100$. The target position on the build plate in this case is represented by the x and y component of the position.

For the investigation of the process limits for the high productive PBF-LB/M process with beam splitter experiments with three different layouts are conducted with standard 316L stainless steel powder with a D90 of 45 µm. A high-quality parameter set with a volumetric energy density of 64.8 J/mm³ is used. Every layout is defined by the spot rotation with different spot rotations of 0°, 45°, and 90° to the x-axis with the goal to investigate the influence of the angle between shielding gas flow and spot orientation. The cubes were positioned in a way that the pattern could be rotated around itself as depicted in Figure 3. This approach yields a multitude of focus errors in the positions of the side beams build cubes. That way, a mix of different focus error and shielding gas flow to spot rotation angles can be examined.

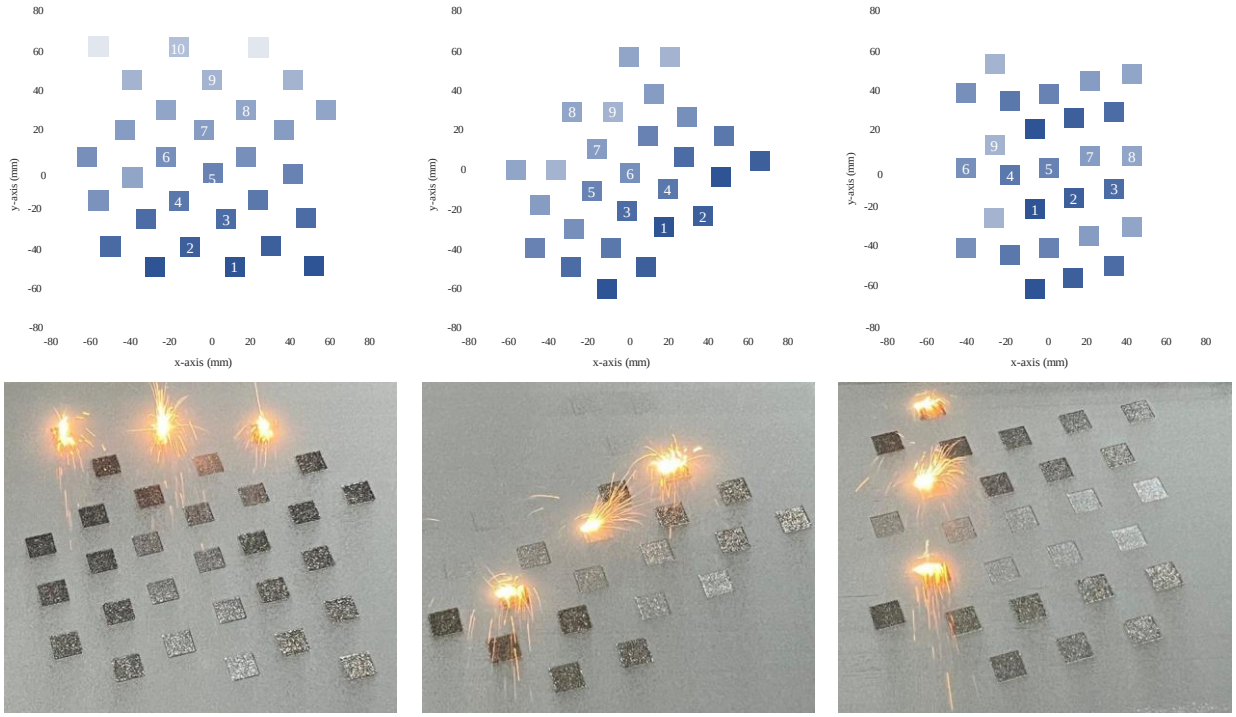

Figure 3: Positions of the 10 mm cubes on the build plate numbered according to their position in the processing sequence for the spot rotations a) 0°, b) 45°, and c) 90°

To analyse the influence of the focus error on the build quality and investigate the process limits the densities of the cubes are measured as an indicator for build quality. This is achieved through the utilisation of the buoyancy method. The scale used possesses a measurement error of

6 mg which leads to a measurement error in the densities of < 0.12%. The surface roughness, measured to further indicate on the build quality is measured using a structured light profilometer with a measurement accuracy of ± 2.5 µm.

Results and Discussion

In the following section the results of the analysis of the influence of the focus error influence on the density and surface roughness are presented and resulting process limits are discussed. Following that the influence of the shielding gas flow is discussed on basis of the results for density and surface roughness, necessary limitations for the process are derived from there. Finally, compensation strategies for focus error and shielding gas flow interactions are discussed.

Focus error

This analysis begins with an examination of the effects of the focus error. In order to isolate the effects of the focus error, all cubes with influences from the shield gas flow, including insufficient shield gas flow velocity and intercube fume interaction, have been excluded from this analysis. This approach ensures that the influence of the focus error is free of additional influences, allowing for a more accurate assessment of its impact. As depicted in Figure 4, a negative correlation of the focus error and density is measured over all spot rotations. In addition to that, an increase in the standard deviation is observable with higher focus errors. This phenomenon is likely to occur due to a reduction in laser beam intensity, which can be attributed to an expansion in the effective beam waist diameter and, consequently, an increase in the illuminated area. This boosts the formation of an unstable welding process with lack of fusion defects due to the low effective energy intensity from the focus error insufficient to keep up a stable melt pool. For the presented process, the first significant decrease in density is visible with a focus error of larger than 20%, while the density threshold of 99.5% is surpassed even with a focus error of 50.7%. This represents a focus diameter of 109 µm representing a reduction of the energy density for the area illuminated by the beam to 43.6% of the energy density for the single beam process. From here two main process limitations concerning the focus error and the density can be derived. On the one hand, printing multiple parts with beam splitting is needs an increase in laser power if the cubes must be as dense as possible, in the presented case for the center beam with a density of 99.9%. Yet on the other hand if a density of 99.5% does meet the specific product specifications, a focus error of up to 50% can be accepted, which limits the usable area on the build plate for the beam multiplication but offers great possibilities for the use of the productivity benefits through parallelisation.

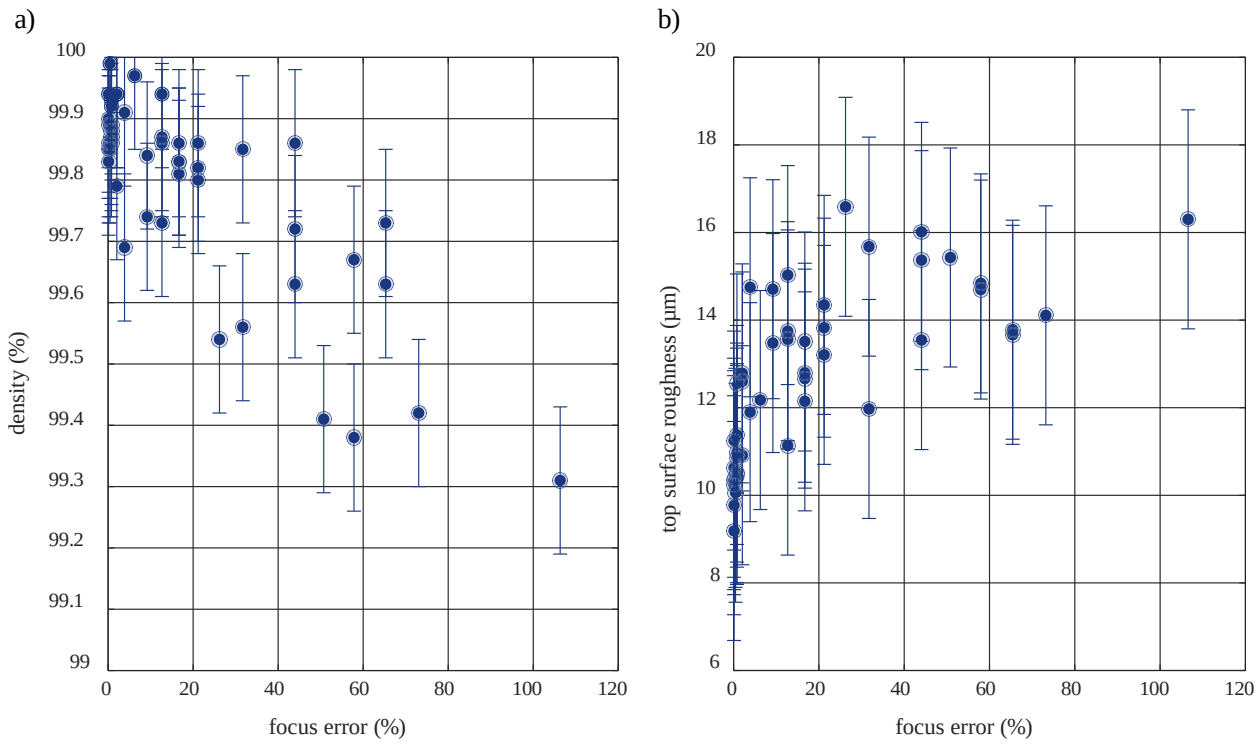

Figure 4: Influence of focus error on a) density and b) top surface roughness of the build parts

In addition, a positive correlation of the surface roughness to the focus error can be observed in Figure 4. This is especially visible for the minimum surface roughness, which increases continuously for increasing focus error. One explanation for this effect could be the lack of fusion defects resulting in higher surface roughness from the defects on the surface as depicted in Figure 5 for an exemplary cube triple built in parallel. While the weld beads for the cube built by the center beam are clearly distinguishable and show little to no defects, the cubes built by the side beams show defects far more frequent and the weld beads are a lot less clear. This indicates a discontinuous melt pool which is frequently collapsing due to Plateau-Rayleigh instability. Additionally, many partial molten particles are visible on the top surface of the cubes build by the side beams increasing the roughness further.

In addition to this, the surface roughness for focus errors below 1% ranges from 9.2 µm up to 12.6 µm and for focus errors lower than 20% up to 16.6 µm, which shows a broad band of roughness for similar focus errors. This leads to the conclusion, that high fluctuations in the surface roughness are not only due to the focus error, but high fluctuation is most likely due to the oxygen content of 0.3 % in the laboratory machine fostering stochastic occurring spatter and fume interactions with the beam resulting in higher surface roughness.

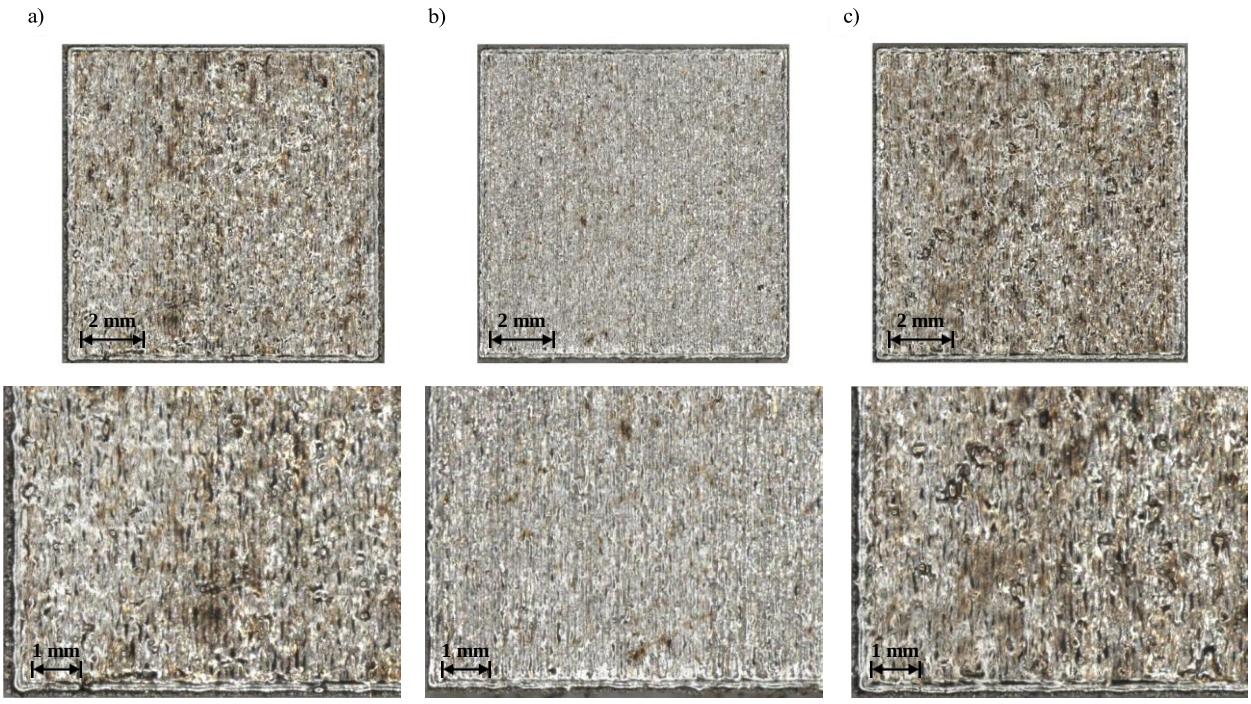

Ra	15 µm	10 µm	17 µm
%	99.73	99.85	99.54

Figure 5: Exemplary microscopic images of order number a) -1, b) 0 and c) +1 for the test specimen 6's surface of the 0°experiment

The resulting process limitation of the focus error for surface roughness are twofold. On the one hand, a low focus error does not guarantee a low surface roughness, yet it shows the lowest measured values. On the other side, the minimal measured surface roughness increases with increasing focus error. This leads to the conclusion, that the focus error should be reduced to zero if the best surface roughness is needed to reduce its influence on the result. If certain compromises concerning the surface roughness can be accomplished, the focus error inherent to the presented high productive process might be tolerable even for higher focus errors and is not the limiting factor for the process. In the presented experiments, the maximum surface roughness does not increase with increasing focus error above a value of 17 µm. Nevertheless, the average surface error increases with increasing focus error. Therefore, a higher number of cubes with high focus errors above 60% would be beneficial for a deeper understanding to what extend the maximum surface roughness is capped at an upper limit independent of the focus error. Although the negative influence on the density would make this approach unnecessary when building quality parts.

Fume interaction

Although the PBF/LB-M process is always associated with spatter and process fumes, in the case of beam multiplication certain questions arise about the interaction of the geometric dependent spots and their resulting process byproduct interaction for certain spot rotations. This influence is especially visible when spots are rotated parallel to the shielding gas flow as depicted in Figure 6. In this case, the process byproducts in the area of the downstream side laser beams alter the laser beam intensity illuminating the melt pool as well as spatters landing on the soon to

be processed powder bed. There is a larger glow above the melt pool can be observed which is to be expected to result from a higher degree of absorption of the beam compared to the perpendicular spot rotation. In the following this is called a direct interaction because the process byproducts directly interact with another laser beam. On contrary, an indirect interaction is considered, when the byproducts land on parts of the build plate which are processed at a later point in time.

a) b)

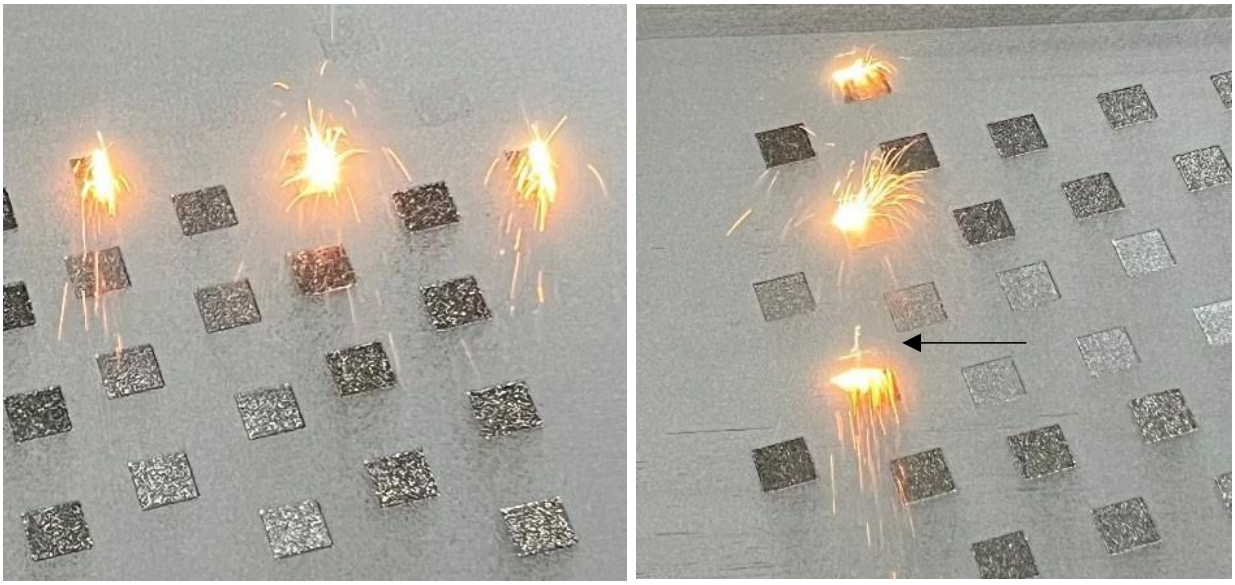

Figure 6: Examples for beam-fume interactions a) no interactions and b) direct interaction of the fumes from the upstream melt pools, while the indirect interactions not visible from the process glow in image

Regarding the experimental analysis of the shielding gas flow velocity, a strong influence on the density of the build parts for velocities smaller than 1.5 m/s is observed with a lower average density of 99.56% compared to the average density of 99.79% for the parts with no shield gas interaction, as depicted in Figure 7. In a reaction to this result these cubes are excluded from the evaluation of intercube fume interaction. Looking at the intercube fume interaction, the average density is measured with 99.76% for all affected cubes. This does not differ much from the cubes with no intercube interactions. But the spread of results increased as well as the standard deviation from 0.16% density to 0.20% with direct intercube fume interaction. These results are likely influenced by the trajectory of the fumes and spatter particles. While the spatter particles from the side beam melt pools show the tendency to fall back on their origin cube, the ones ejected from the center beam melt pool have a far more up right trajectory probably leading to a transportation of the spatter to the downstream beam.

The findings are similar for the influence of the shielding gas flow on the top surface roughness. The biggest roughness with an average of 15 µm is observed when the shielding gas flow velocity drops below 1.5 m/s. Yet the average roughness with and without intercube fume interaction remains similar, but the standard deviation increased with direct interactions. The indirect interaction is showing smaller effects compared to the no interaction dataset. The averages for density and surface roughness are similar. Although the improvement in lower deviation is best explained by the lower number of test samples compared to the no interaction dataset.

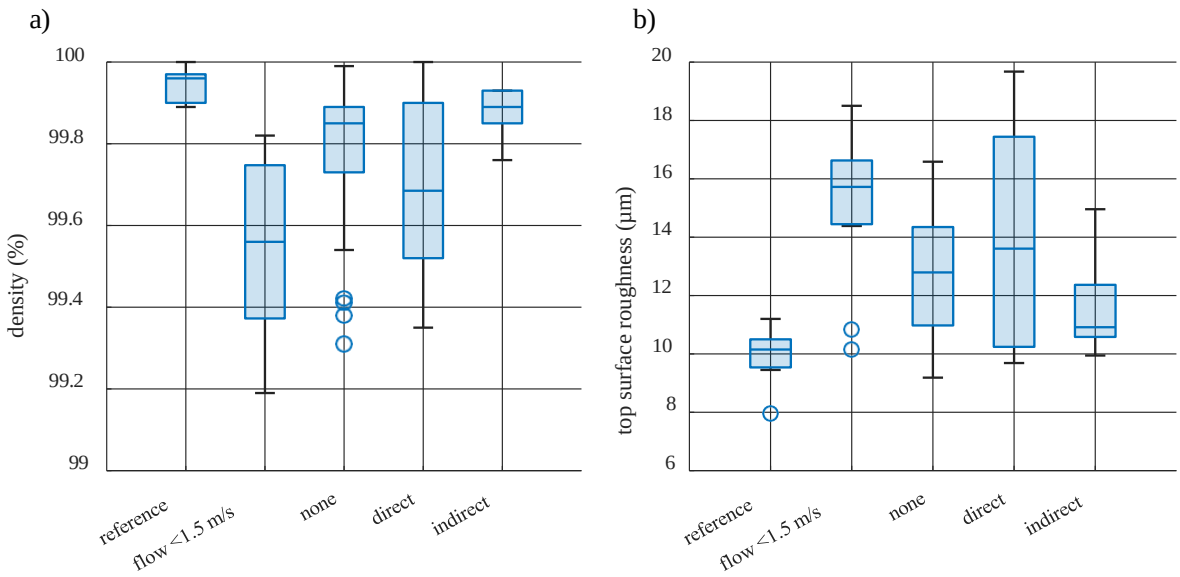

Figure 7: Influence of shielding gas flow on a) density and b) surface roughness of the build parts separated in reference parts build with a single laser beam (n=11), parts with a shield gas flow <1.5 m/s (n=11) and without (n=46), direct (n=18) and indirect (n=8) intercube fume interaction

Regarding the process limits for fume interaction, the understanding is that interaction is to be completely avoided, which means the cubes have to be rotated to less than the fume interaction area and all cubes need a shielding gas flow velocity of over 1.5 m/s. Nevertheless, both measures result in different impacts on the quality parameters. It is observed, that while the low shielding gas velocity needs to be avoided because of its negative effects on the averages of densities roughness, the intercube fume interactions need to be avoided to decrease their stochastic effects resulting in higher fluctuation of density and top surface roughness. One step further, investigating the indirect fume interaction compared to direct interaction only a small effect on the top surface roughness can be measured.

Compensation

Both influences, the focus error, and the shielding gas flow, show effects on the density and top surface roughness of the built specimens. Thereby both need to be compensated to enable processing inside the explored process limits. Looking at the shielding gas flow, the main goal should be to ensure a process zone for all parallel beams as free as possible from any process emissions. On the one hand the spot rotation has to be optimised concerning the angle to the shielding gas flow to ensure the efficient evacuation of the fumes and spatters away from the processing zones of the laser beams. This could be achieved by the layout of the print job. On the other hand, a compensation with an improved shielding gas flow solves this issue. Due to the influence of energy density in correlation with the focus error on the density of parts it is of important to minimize the focus error with mitigation strategies. This could be achieved by deliberately defocusing the center beam, accepting an increase in focus error for the center beam while decreasing the focus error for the side beams, as depicted in Figure 8. Nevertheless, this compensation strategy is not sufficient for a total compensation of the focus error and thereby not feasible for quality requirements demanding the best possible density and top surface roughness.

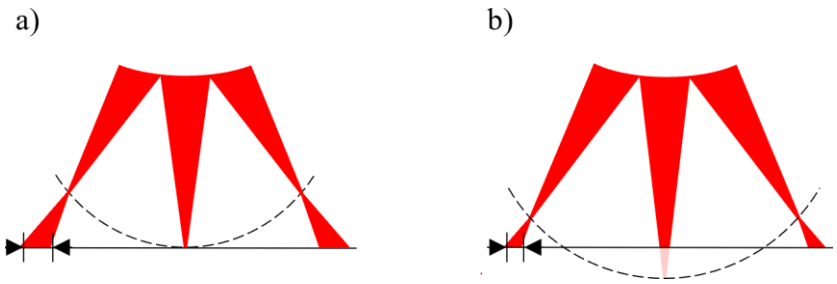

Figure 8: Schematic overview of a) the regular focus level of the beam and b) the compensated beam for less focus error

Conclusions

A beam splitter in form of a DOE was used in the presented work to multiplicate the parts built with one laser scanner system. Due to the inherent optical errors and the geometric dependency of the single spots the process limits were investigated. Therefore, three experimental build job layouts were conducted with different focus errors, resulting from different effective waist beam diameters and three discrete spot rotations depending on the shield gas flow direction. These experiments were analysed on their density and their top surface roughness.

Both influences show effects on the parameters, but in different ways. On the one hand an increase in focus error resulted in a lower average density of 99.7% and higher minimal surface roughness and additional increasing the variance of both. On the other hand, the intercube shielding gas influences mainly resulted in a higher variance. The results of this study have led to the identification of process limitations. These include the avoidance of fumes from other cubes to interact downstream with another laser beam and to not work with focus errors exceeding 50%. In conclusion, the higher the tolerances for density and top surface roughness the better beam multiplication can be used to increase the productivity. Furthermore, the presented compensation strategies could be used to further increase the area of deployment for this technology.

Acknowledgements

The shown results have been supported by the work of Danai Bersou, Johannes Moesbauer and Julia Stein.

References

[1] M. Slodczyk, A. Ilin, T. Kiedrowski, T. Bareth, V. Ploshikhin, Spatter reduction by multi-beam illumination in laser powder-bed fusion, Materials & Design 212 (2021) 110206. https://doi.org/10.1016/j.matdes.2021.110206.

[2] C.-Y. Tsai, C.-W. Cheng, A.-C. Lee, M.-C. Tsai, Synchronized multi-spot scanning strategies for the laser powder bed fusion process, Additive Manufacturing 27 (2019) 1–7. https://doi.org/10.1016/j.addma.2019.02.009.

[3] F. J. O. Spieth, T. Heeling, H.-C. Moehring, Influences of optical errors in the SLM process with high separation angle beam splitting (2023) in: lasers in manufacturing conference proceedings.

[4] L. Büsing, Optische Systeme für die hochpräzise, scannerbasierte Multistrahlbearbeitung mit ultrakurzen Laserpulsen. dissertation, Aachen, 2016.
[5] X. Nie, Z. Chen, Y. Qi, H. Zhang, C. Zhang, Z. Xiao, H. Zhu, Effect of defocusing distance on laser powder bed fusion of high strength Al–Cu–Mg–Mn alloy, Virtual and Physical Prototyping 15 (2020) 325–339. https://doi.org/10.1080/17452759.2020.1760895.
[6] J.P. Oliveira, A.D. LaLonde, J. Ma, Processing parameters in laser powder bed fusion metal additive manufacturing, Materials & Design 193 (2020) 108762. https://doi.org/10.1016/j.matdes.2020.108762.
[7] M.C. Sow, T. de Terris, O. Castelnau, Z. Hamouche, F. Coste, R. Fabbro, P. Peyre, Influence of beam diameter on Laser Powder Bed Fusion (L-PBF) process, Additive Manufacturing 36 (2020) 101532. https://doi.org/10.1016/j.addma.2020.101532.
[8] B. Liu, G. Fang, L. Lei, W. Liu, Experimental and numerical exploration of defocusing in Laser Powder Bed Fusion (LPBF) as an effective processing parameter, Optics & Laser Technology 149 (2022) 107846. https://doi.org/10.1016/j.optlastec.2022.107846.
[9] T. Grünberger, R. Domröse, Direct Metal Laser Sintering, Laser Technik Journal 12 (2015) 45–48. https://doi.org/10.1002/latj.201500007.
[10] J. Greses, P.A. Hilton, C.Y. Barlow, W.M. Steen, Plume attenuation under high power Nd:yttritium–aluminum–garnet laser welding, Journal of Laser Applications 16 (2004) 9–15. https://doi.org/10.2351/1.1642636.
[11] A. Ladewig, G. Schlick, M. Fisser, V. Schulze, U. Glatzel, Influence of the shielding gas flow on the removal of process by-products in the selective laser melting process, Additive Manufacturing 10 (2016) 1–9. https://doi.org/10.1016/j.addma.2016.01.004.
[12] Z. Sun, X. Tan, S.B. Tor, Effects Of Chamber Oxygen Concentration On The Microstructure And Mechanical Properties Of Selective Laser Melting Built Stainless Steel 316L, Nanyang Technological University, 2018.
[13] B. Ferrar, L. Mullen, E. Jones, R. Stamp, C.J. Sutcliffe, Gas flow effects on selective laser melting (SLM) manufacturing performance, Journal of Materials Processing Technology 212 (2012) 355–364. https://doi.org/10.1016/j.jmatprotec.2011.09.020.
[14] O. Andreau, I. Koutiri, P. Peyre, J.-D. Penot, N. Saintier, E. Pessard, T. de Terris, C. Dupuy, T. Baudin, Texture control of 316L parts by modulation of the melt pool morphology in selective laser melting, Journal of Materials Processing Technology 264 (2019) 21–31. https://doi.org/10.1016/j.jmatprotec.2018.08.049.
[15] Di Wang, S. Wu, F. Fu, S. Mai, Y. Yang, Y. Liu, C. Song, Mechanisms and characteristics of spatter generation in SLM processing and its effect on the properties, Materials & Design 117 (2017) 121–130. https://doi.org/10.1016/j.matdes.2016.12.060.
[16] C. Tenbrock, T. Kelliger, N. Praetzsch, M. Ronge, L. Jauer, J.H. Schleifenbaum, Effect of laser-plume interaction on part quality in multi-scanner Laser Powder Bed Fusion, Additive Manufacturing 38 (2021) 101810. https://doi.org/10.1016/j.addma.2020.101810.